

Singlet scalar Dark matter in $U(1)_{B-L}$ models without right-handed neutrinos

Shivaramakrishna Singirala,^{1,*} Rukmani Mohanta,^{1,†} and Sudhanwa Patra^{2,‡}

¹*School of Physics, University of Hyderabad, Hyderabad - 500046, India*

²*Indian Institute of Technology Bhilai, GEC Campus,
Sejbahar, Raipur-492015, Chhattisgarh, India*

Abstract

We investigate the phenomenology of singlet scalar dark matter in a simple $B-L$ gauge extension of the Standard Model where the dark matter particle is charged under the $U(1)_{B-L}$ symmetry. The non-trivial gauge anomalies are cancelled with the introduction of three exotic fermions with $B-L$ charges as $-4, -4, 5$, instead of right-handed neutrinos ν_{Ri} ($i = 1, 2, 3$) with $B-L = -1$ in conventional $U(1)_{B-L}$ model. Without the need of any ad-hoc discrete symmetry, the $B-L$ charge plays a crucial role in stabilizing the dark matter. We make a comprehensive study of dark matter phenomenology in the scalar and gauge portals separately. In the gauge-mediated regime, we invoke the LEP-II constraints and dilepton limits of ATLAS on the gauge parameters. A massless physical Goldstone plays a vital role in the scalar-portal dark matter observables, becomes a unique feature of the model. We show the mechanism of generating the light neutrino mass at one-loop level where the dark matter singlet runs in the loop. We shed light on the semi-annihilation and finally, we comment on indirect signals in this framework.

arXiv:1704.01107v2 [hep-ph] 8 Nov 2018

*Electronic address: krishnas542@gmail.com

†Electronic address: rmsp@uohyd.ernet.in

‡Electronic address: sudhanwa@iitbhilai.ac.in

I. INTRODUCTION

Although there are indirect astrophysical evidences for the existence of dark matter contributing with a relic density $\Omega h^2 \simeq 0.12$, about 25% to the energy budget of the Universe [1], still we know only very little about the nature of the dark matter. In particular the unknowns are: what kind of particle it is, i.e., scalar, fermion or vector etc., and to which beyond the Standard Model framework it belongs to (see the recent review article [2] for details). In this respect, models in which the difference between baryon and lepton number ($B - L$) is gauged, are economic extensions of the Standard Model [3–6] (see also few earlier works in this direction [7–15]). One of the interesting aspects of this kind of models is that in the standard form, the presence of right-handed neutrinos and thus, the type-I seesaw mechanism for neutrino mass generation appears naturally. In addition, attempts have also been made within this economic extensions of SM where dark matter can be incorporated as well [16–26].

It is widely believed that weakly interacting massive particles (WIMPs) fulfil the necessary criteria of dark matter, not too far from the electroweak scale, which provides the opportunity to test them at the current or near future direct or indirect dark matter detection experiments. One of the fundamental questions is how to address the stability of the dark matter. Within the gauged $B - L$ extensions of the Standard Model, the stability of the dark matter can be taken care of by imposing an extra discrete symmetry on top of the gauge symmetry [19–21, 24]. In these class of models one of the right-handed neutrinos introduced for gauge anomaly cancellation is odd under the additional discrete symmetry and acts as a dark matter candidate. Attempts are also made to ensure the stability of the dark matter by choosing the appropriate $B - L$ charge of dark matter [17, 18, 22, 23, 25]. There are other variants of gauged $B - L$ extension of SM, where the additional fermions carry exotic integer value of $B - L$ charge. The discussion of scalar dark matter and neutrino phenomenology have been explored in the recent works [27–29], while a beautiful connection between dark matter abundance and matter-antimatter asymmetry has been investigated in Ref. [25] within WIMPy Leptogenesis.

In this work, we attempt to study the phenomenology of a scalar dark matter within the context of gauged $B - L$ model without the introduction of any right-handed neutrinos, which are generally present in the conventional $B - L$ theory. The induced gauge anomalies are cancelled by assigning appropriate $B - L$ charges to the additional fermions. The key point to note here is that the stability of the scalar singlet dark matter is ensured by the peculiar choice of $B - L$ charges and not by introducing any ad-hoc discrete symmetry. The proposed model provides another variant of the class of gauged $B - L$ models. Similar work on singlet scalar DM phenomenology has been recently explored in [17] where three right-handed neutrinos are added to make the model anomaly free and the model structure itself takes care of the stability of scalar DM. Dirac DM has also recently been investigated in a $B - L$ model [30], where four exotic fermions are added to overcome the gauge anomalies. The current model describes a new variant of $B - L$ models with a different scalar content and exotic charges assigned to the newly added fermions. Moreover, the $B - L$ charge assigned to the scalar DM and its corresponding annihilation channels, the arising parameter scan

are different from the conventional $B - L$ models.

The plan of the paper is as follows. We discuss in Sec-II, a simple model with $B - L$ gauge extension of SM without right-handed neutrinos along with the allowed solutions for gauge anomaly cancellation, vacuum stability criteria, perturbative unitarity constraints and the mass spectrum of the scalar sector. In Sec-III, we explore the Z' -mediated dark matter phenomenology of scalar singlet in view of relic density, direct detection and collider bounds perspective. In Sec-IV, we repeat the same for the scalar-portal, then we briefly discuss the generation of light neutrino mass and the effect of semi-annihilation to relic density in Sec-V and VI respectively. In Sec-VII, we comment on indirect signals followed by conclusion in Sec-VIII.

II. THE MODEL FRAMEWORK

It is believed that the $B - L$ gauge extension of Standard Model (SM) is the simplest model one can think of from the point of view of a self-consistent gauge theory where the difference between baryon and lepton number is promoted to local gauge symmetry. The gauge group of this simplest $B - L$ model is $SU(2)_L \times U(1)_Y \times U(1)_{B-L}$, omitting the $SU(3)_C$ structure for simplicity. Originally, these models are motivated to cancel the triangle gauge anomalies

$$\mathcal{A}_1 [U(1)_{B-L}^3], \quad \mathcal{A}_2 [(\text{gravity})^2 \times U(1)_{B-L}], \quad (1)$$

with the inclusion of right-handed neutrinos ν_{Ri} ($i = 1, 2, 3$) having the $B - L$ charges -1 (the other gauge anomalies, i.e., $\mathcal{A}_3 [SU(3)_C^2 \times U(1)_{B-L}]$ and $\mathcal{A}_4 [SU(2)_L^2 \times U(1)_{B-L}]$ trivially cancel). These right-handed neutrinos can generate light neutrino masses via the type-I seesaw mechanism [31–34] and account for matter-antimatter asymmetry of the universe. However, we present below few other possible solutions to overcome these anomalies.

A. Anomaly cancellation with additional fermions having exotic B-L charges

In order to build an anomaly free $B - L$ gauge extended framework, the charges of the additional fermion content have to satisfy two simple equations given as [35]

$$\sum_{i=1}^{n_R} x_i^3 = 3 \quad \text{and} \quad \sum_{i=1}^{n_R} x_i = 3, \quad (2)$$

where n_R denotes the number of additional fermions and x_i denotes the $B - L$ charge of each fermion. $n_R = 1$ gives no solution and $n_R = 2$ gives a complex solution. $n_R \geq 3$ is always suitable to have real solutions. For instance, choosing the charges as $-4, -4$ and $+5$ is one such solution satisfying 2 and has been explored in [27, 28]. We show below the explicit check

$$\begin{aligned} \mathcal{A}_1 [U(1)_{B-L}^3] &= \mathcal{A}_1^{\text{SM}} (U(1)_{B-L}^3) + \mathcal{A}_1^{\text{New}} (U(1)_{B-L}^3) = -3 + (4^3 + 4^3 + (-5)^3) = 0, \\ \mathcal{A}_2 [\text{gravity}^2 \times U(1)_{B-L}] &\propto \mathcal{A}_2^{\text{SM}} (U(1)_{B-L}) + \mathcal{A}_2^{\text{New}} (U(1)_{B-L}) = -3 + (4 + 4 + (-5)) = 0. \end{aligned}$$

There could also be a different solution to cancel the gauge anomalies, where one requires four additional fermions carrying fractional $B - L$ charges (first proposed in

	Field	$SU(2)_L \times U(1)_Y$	$U(1)_{B-L}$
Fermions	$Q_L \equiv (u, d)_L^T$	$(\mathbf{2}, 1/6)$	$1/3$
	u_R	$(\mathbf{1}, 2/3)$	$1/3$
	d_R	$(\mathbf{1}, -1/3)$	$1/3$
	$\ell_L \equiv (\nu, e)_L^T$	$(\mathbf{2}, -1/2)$	-1
	e_R	$(\mathbf{1}, -1)$	-1
	N_{1R}	$(\mathbf{1}, 0)$	-4
	N_{2R}	$(\mathbf{1}, 0)$	-4
	N_{3R}	$(\mathbf{1}, 0)$	5
Scalars	H	$(\mathbf{2}, 1/2)$	0
	ϕ_{DM}	$(\mathbf{1}, 0)$	n_{DM}
	ϕ_1	$(\mathbf{1}, 0)$	-1
	ϕ_8	$(\mathbf{1}, 0)$	8

TABLE I: Particle spectrum and their charges of the proposed $U(1)_{B-L}$ model.

Ref. [30]). We briefly describe below, how the non-trivial gauge anomalies $\mathcal{A}_1 (U(1)_{B-L}^3)$ and $\mathcal{A}_2 (\text{gravity}^2 \times U(1)_{B-L})$ get cancelled by introducing four exotic fermions with fractional $B-L$ charges, i.e., $\xi_L(4/3)$, $\eta_L(1/3)$, $\chi_{1R}(-2/3)$ and $\chi_{2R}(-2/3)$, where the corresponding $B-L$ charges are shown in the parenthesis,

$$\begin{aligned}
\mathcal{A}_1 [U(1)_{B-L}^3] &= \mathcal{A}_1^{\text{SM}} (U(1)_{B-L}^3) + \mathcal{A}_1^{\text{New}} (U(1)_{B-L}^3) \\
&= -3 + \left[\left(\frac{4}{3}\right)^3 + \left(\frac{1}{3}\right)^3 + \left(\frac{2}{3}\right)^3 + \left(\frac{2}{3}\right)^3 \right] = 0, \\
\mathcal{A}_2 [\text{gravity}^2 \times U(1)_{B-L}] &\propto \mathcal{A}_2^{\text{SM}} (U(1)_{B-L}) + \mathcal{A}_2^{\text{New}} (U(1)_{B-L}) \\
&= -3 + \left[\left(\frac{4}{3}\right) + \left(\frac{1}{3}\right) + \left(\frac{2}{3}\right) + \left(\frac{2}{3}\right) \right] = 0.
\end{aligned}$$

In this work, we consider the first category of anomaly free model built up based on $U(1)_{B-L}$ extension of the standard model which includes three neutral exotic fermions N_{iR} (where $i = 1, 2, 3$), with the $B-L$ charges $-4, -4$ and $+5$. We include two more scalar singlets ϕ_1 and ϕ_8 to provide Majorana masses for all the exotic fermions and also to spontaneously break the $B-L$ gauge symmetry. We also introduce a scalar dark matter ϕ_{DM} , singlet under the SM gauge group but charged under $U(1)_{B-L}$. It doesn't get any VEV, it does flow in the loop to generate light neutrino mass as discussed in Section-V. Fermionic dark matter of the current model has been explored in [36]. The particle content of the present model is given in Table I.

The relevant terms in the Lagrangian for fermions in the present model is given by

$$\begin{aligned}
\mathcal{L}_{\text{Kin.}}^{\text{fermion}} = & \overline{Q}_L i\gamma^\mu \left(\partial_\mu + ig\frac{\vec{\tau}}{2} \cdot \vec{W}_\mu + \frac{1}{6}ig' B_\mu + \frac{1}{3}ig_{\text{BL}} Z'_\mu \right) Q_L \\
& + \overline{u}_R i\gamma^\mu \left(\partial_\mu + \frac{2}{3}ig' B_\mu + \frac{1}{3}ig_{\text{BL}} Z'_\mu \right) u_R \\
& + \overline{d}_R i\gamma^\mu \left(\partial_\mu - \frac{1}{3}ig' B_\mu + \frac{1}{3}ig_{\text{BL}} Z'_\mu \right) d_R \\
& + \overline{\ell}_L i\gamma^\mu \left(\partial_\mu + ig\frac{\vec{\tau}}{2} \cdot \vec{W}_\mu - \frac{1}{2}ig' B_\mu - ig_{\text{BL}} Z'_\mu \right) \ell_L \\
& + \overline{e}_R i\gamma^\mu \left(\partial_\mu - ig' B_\mu - ig_{\text{BL}} Z'_\mu \right) e_R \\
& + \overline{N}_{1R} i\gamma^\mu \left(\partial_\mu - 4ig_{\text{BL}} Z'_\mu \right) N_{1R} + \overline{N}_{2R} i\gamma^\mu \left(\partial_\mu - 4ig_{\text{BL}} Z'_\mu \right) N_{2R} \\
& + \overline{N}_{3R} i\gamma^\mu \left(\partial_\mu + 5ig_{\text{BL}} Z'_\mu \right) N_{3R} .
\end{aligned} \tag{3}$$

The interaction Lagrangian for the scalar sector is as follows

$$\begin{aligned}
\mathcal{L}_{\text{scalar}} = & (\mathcal{D}_\mu H)^\dagger (\mathcal{D}^\mu H) + (\mathcal{D}_\mu \phi_{\text{DM}})^\dagger (\mathcal{D}^\mu \phi_{\text{DM}}) + (\mathcal{D}_\mu \phi_1)^\dagger (\mathcal{D}^\mu \phi_1) \\
& + (\mathcal{D}_\mu \phi_8)^\dagger (\mathcal{D}^\mu \phi_8) - V(H, \phi_{\text{DM}}, \phi_1, \phi_8) ,
\end{aligned} \tag{4}$$

where the covariant derivatives are

$$\begin{aligned}
\mathcal{D}_\mu H &= \partial_\mu H + ig\vec{W}_{\mu L} \cdot \frac{\vec{\tau}}{2} H + i\frac{g'}{2} B_\mu H , \\
\mathcal{D}_\mu \phi_{\text{DM}} &= \partial_\mu \phi_{\text{DM}} + in_{\text{DM}} g_{\text{BL}} Z'_\mu \phi_{\text{DM}} , \\
\mathcal{D}_\mu \phi_1 &= \partial_\mu \phi_1 - ig_{\text{BL}} Z'_\mu \phi_1 , \\
\mathcal{D}_\mu \phi_8 &= \partial_\mu \phi_8 + 8ig_{\text{BL}} Z'_\mu \phi_8 .
\end{aligned} \tag{5}$$

The Yukawa interaction for the present model is given by

$$\begin{aligned}
\mathcal{L}_{\text{Yuk}} = & Y_u \overline{Q}_L \tilde{H} u_R + Y_d \overline{Q}_L H d_R + Y_e \overline{\ell}_L H e_R \\
& + \sum_{\alpha=1,2} h_{\alpha 3} \phi_1 \overline{N}_{\alpha R}^c N_{3R} + \sum_{\alpha,\beta=1,2} h_{\alpha\beta} \phi_8 \overline{N}_{\alpha R}^c N_{\beta R} ,
\end{aligned} \tag{6}$$

with $\tilde{H} = i\sigma_2 H^*$. From the above Yukawa interaction terms, one can write the exotic fermion mass matrix and diagonalize it to obtain non-zero masses to all the Majorana mass eigenstates.

B. Scalar Potential Minimization and Stability criteria

The scalar potential of this model is given by

$$\begin{aligned}
V(H, \phi_{\text{DM}}, \phi_1, \phi_8) = & \mu_H^2 H^\dagger H + \lambda_H (H^\dagger H)^2 + \mu_1^2 \phi_1^\dagger \phi_1 + \lambda_1 (\phi_1^\dagger \phi_1)^2 + \mu_8^2 \phi_8^\dagger \phi_8 + \lambda_8 (\phi_8^\dagger \phi_8)^2 \\
& + \mu_{\text{DM}}^2 \phi_{\text{DM}}^\dagger \phi_{\text{DM}} + \lambda_{\text{DM}} (\phi_{\text{DM}}^\dagger \phi_{\text{DM}})^2 + \lambda_{\text{H1}} (H^\dagger H) (\phi_1^\dagger \phi_1) + \lambda_{\text{H8}} (H^\dagger H) (\phi_8^\dagger \phi_8) \\
& + \lambda_{18} (\phi_1^\dagger \phi_1) (\phi_8^\dagger \phi_8) + \lambda_{\text{HD}} (H^\dagger H) (\phi_{\text{DM}}^\dagger \phi_{\text{DM}}) + \lambda_{\text{D1}} (\phi_{\text{DM}}^\dagger \phi_{\text{DM}}) (\phi_1^\dagger \phi_1) \\
& + \lambda_{\text{D8}} (\phi_{\text{DM}}^\dagger \phi_{\text{DM}}) (\phi_8^\dagger \phi_8) ,
\end{aligned} \tag{7}$$

where $\phi_{\text{DM}} = \frac{S+iA}{\sqrt{2}}$, the scalar fields $H = (H^+, H^0)^T$, ϕ_1 and ϕ_8 can be parametrized in terms of real scalars and pseudo scalars as

$$\begin{aligned} H^0 &= \frac{1}{\sqrt{2}}(v+h) + \frac{i}{\sqrt{2}}A^0, \\ \phi_1^0 &= \frac{1}{\sqrt{2}}(v_1+h_1) + \frac{i}{\sqrt{2}}A_1, \\ \phi_8^0 &= \frac{1}{\sqrt{2}}(v_8+h_8) + \frac{i}{\sqrt{2}}A_8, \end{aligned} \quad (8)$$

where $\langle H \rangle = (0, v/\sqrt{2})^T$, $\langle \phi_1 \rangle = v_1/\sqrt{2}$, and $\langle \phi_8 \rangle = v_8/\sqrt{2}$.

C. Vacuum stability criteria and Unitarity constraints

The vacuum stability conditions of the scalar potential are given by [37, 38]

$$\begin{aligned} \lambda_H &\geq 0, \quad \lambda_{\text{HD}} \geq 0, \quad \lambda_{\text{DM}} \geq 0, \quad \lambda_1 \geq 0, \quad \lambda_8 \geq 0, \\ \lambda_{\text{D1}} + \sqrt{\lambda_{\text{DM}}\lambda_1} &\geq 0, \quad \lambda_{\text{D8}} + \sqrt{\lambda_{\text{DM}}\lambda_8} \geq 0, \quad \lambda_{18} + \sqrt{\lambda_1\lambda_8} \geq 0, \\ \sqrt{\lambda_{\text{DM}}\lambda_1\lambda_8} + \lambda_{\text{D1}}\sqrt{\lambda_8} + \lambda_{\text{D8}}\sqrt{\lambda_1} + \lambda_{18}\sqrt{\lambda_{\text{DM}}} &\geq 0. \end{aligned} \quad (9)$$

Now we apply the tree-level perturbative unitarity constraints on the scattering processes of the scalar sector. The formula for the zeroth partial wave amplitude [39] is given by

$$a_0 = \frac{1}{32\pi} \sqrt{\frac{4p_f^{\text{CM}} p_i^{\text{CM}}}{s}} \int_{-1}^{+1} d(\cos\theta) T_{2 \rightarrow 2}. \quad (10)$$

Here $p_{i,(f)}^{\text{CM}}$ is the the centre of mass (CoM) momentum of the initial (final) state, s is the (CoM) energy, and $T_{2 \rightarrow 2}$ denotes the full amplitude of each $2 \rightarrow 2$ scattering processes. At high energies, the partial wave amplitudes i.e., the quartic couplings gets constrained from perturbative unitarity requirement $|\text{Re}(a_0)| \leq \frac{1}{2}$, giving

$$\begin{aligned} \lambda_H, \lambda_1, \lambda_8, \lambda_{\text{DM}} &\leq \frac{4\pi}{3}, \\ \lambda_{\text{HD}}, \lambda_{\text{D1}}, \lambda_{\text{D8}}, \lambda_{\text{H1}}, \lambda_{\text{H8}}, \lambda_{18} &\leq 4\pi. \end{aligned} \quad (11)$$

D. Mixing in scalar sector

In the scalar sector, the CP-even scalar mass matrix takes the form

$$M_E^2 = \begin{pmatrix} 2\lambda_H v^2 & \lambda_{\text{H1}} v v_1 & \lambda_{\text{H8}} v v_8 \\ \lambda_{\text{H1}} v v_1 & 2\lambda_1 v_1^2 & \lambda_{18} v_1 v_8 \\ \lambda_{\text{H8}} v v_8 & \lambda_{18} v_1 v_8 & 2\lambda_8 v_8^2 \end{pmatrix}. \quad (12)$$

We assume that the Higgs doublet H mixes equally with the two singlets and the mixing is small so that the decay width of Higgs is consistent with LHC limits. We also consider the

VEVs of the new singlets $v_1 \simeq v_8 \gg v$ and the couplings $\lambda_{H_1, H_8} \ll \lambda_H$, $\lambda_1 \simeq \lambda_8$ then the mass matrix takes a simple form

$$M_E^2 \simeq \begin{pmatrix} a & a & a \\ a & y & b \\ a & b & y \end{pmatrix}. \quad (13)$$

Under the assumption of minimal Higgs mixing, the unitary matrix that connects the flavor and mass states is

$$U \simeq \begin{pmatrix} 1 & \beta \cos \alpha - \beta \sin \alpha & \beta \cos \alpha + \beta \sin \alpha \\ -\beta & \cos \alpha & \sin \alpha \\ -\beta & -\sin \alpha & \cos \alpha \end{pmatrix}. \quad (14)$$

Here $\beta = \frac{a}{b+y-a}$ is the mixing parameter for $H - \phi_{1,8}$ and $\alpha = \frac{5\pi}{4}$ denotes $\phi_1 - \phi_8$ mixing, obtained from the normalized eigenvector matrix of M_E^2 (13). Thus, the relation between flavor and mass eigenstates is given by

$$\begin{pmatrix} h \\ h_1 \\ h_8 \end{pmatrix} = U \begin{pmatrix} H_1 \\ H_2 \\ H_3 \end{pmatrix} = \begin{pmatrix} H_1 - H_3 \beta \sqrt{2} \\ -H_1 \beta - \frac{H_2}{\sqrt{2}} - \frac{H_3}{\sqrt{2}} \\ -H_1 \beta + \frac{H_2}{\sqrt{2}} - \frac{H_3}{\sqrt{2}} \end{pmatrix}. \quad (15)$$

The scalar couplings can be written as

$$\begin{aligned} 2\lambda_H v^2 &= \lambda_{H_1} v v_1 = \frac{M_{H_1}^2}{(1 - 2\beta + 2\beta^2)}, \\ 2\lambda_1 v_1^2 &= 2\lambda_8 v_8^2 = \frac{(\beta + 1)M_{H_3}^2 + (1 + \beta + 4\beta^2)M_{H_2}^2}{2(1 + \beta + 4\beta^2)}, \\ \lambda_{18} v_1 v_8 &= \frac{(\beta + 1)M_{H_3}^2 - (1 + \beta + 4\beta^2)M_{H_2}^2}{2(1 + \beta + 4\beta^2)}. \end{aligned} \quad (16)$$

Here H_1 denotes the SM Higgs with $M_{H_1} = 125.09$ GeV with $v = 246$ GeV. The mixing angle β can be written in terms of the physical scalar masses as

$$\beta = \frac{-M_{H_1}^2 + M_{H_3}^2 - \sqrt{-15M_{H_1}^4 - 10M_{H_3}^2 M_{H_1}^2 + M_{H_3}^4}}{4(2M_{H_1}^2 + M_{H_3}^2)}. \quad (17)$$

Since the Higgs mass (M_{H_1}) is fixed, the mass parameter M_{H_3} defines the amount of mixing i.e., say $M_{H_3} \geq 1$ TeV implies $\beta \leq 0.016$. Moving to CP-odd components, the linear combination (denoted by A_G) of A_1 and A_8 is eaten up by Z' and the other orthogonal combination, A_{NG} remains as a massless physical Goldstone (NG), which are given by

$$\begin{aligned} A_G &= -\frac{8v_8}{\sqrt{v_1^2 + 64v_8^2}} A_8 + \frac{v_1}{\sqrt{v_1^2 + 64v_8^2}} A_1, \\ A_{NG} &= \frac{v_1}{\sqrt{v_1^2 + 64v_8^2}} A_8 + \frac{8v_8}{\sqrt{v_1^2 + 64v_8^2}} A_1. \end{aligned} \quad (18)$$

As per the assumption $v_1 \simeq v_8$, one can see that A_G gets major contribution from A_8 and A_{NG} is maximally composed of A_1 . This massless mode can couple to the new fermion and

scalar sectors as shown in Appendix A. In SM, it can only couple to Higgs as we considered non-zero mixing between H and the new scalar singlets. It can give rise to an additional decay channel contributing to the invisible width of SM Higgs, given as

$$\Gamma(H_1 \rightarrow A_{\text{NG}}A_{\text{NG}}) \simeq \frac{M_{H_1}^3 \sin^2 \beta}{32\pi} \left(\frac{v_1^3 + 64v_8^3}{v_1 v_8 (v_1^2 + 64v_8^2)} \right)^2, \quad (19)$$

where β denotes the mixing between H and ϕ_1 . The invisible branching ratio of Higgs is given as

$$\text{Br}_{\text{inv}} = \frac{\Gamma(H_1 \rightarrow A_{\text{NG}}A_{\text{NG}})}{\Gamma(H_1 \rightarrow A_{\text{NG}}A_{\text{NG}}) + \cos^2 \beta \Gamma_{\text{SM}}^{\text{Higgs}}}. \quad (20)$$

Using the constraint, $\text{Br}_{\text{inv}} \simeq 20\%$ [40, 41], $\Gamma_{\text{SM}}^{\text{Higgs}} \simeq 4 \text{ MeV}$, we obtain the upper limit on the mixing angle as

$$|\tan \beta| \lesssim 2.2 \times 10^{-4} \times \left(\frac{v_1}{\text{GeV}} \right). \quad (21)$$

Moreover, if the NG stays in thermal equilibrium with ordinary matter until muon annihilation, then it mimics as fractional cosmic neutrinos contributing nearly 0.39 to the effective number of neutrino species [42] to give $N_{\text{eff}} = 3.36_{-0.64}^{+0.68}$ at 95% C.L., a remarkable agreement with Planck data. This illustration was done by working in the low mass regime of the physical scalar ($\simeq 500 \text{ MeV}$). However, in the present work, we consider higher mass regime for the physical scalar spectrum and discuss the effect of NG on relic density in the upcoming section.

E. Stability of singlet scalar dark matter

Dark matter particle has to be electrically neutral and should be stable over cosmological time scales. With this motivation numerous frameworks were proposed based on an unbroken discrete symmetry [43, 44] forbidding the decay of DM. Furthermore, this discrete symmetry is expected to break at Planck scale and thus, induce the decay of DM making it unstable. In the present model, we don't assume any ad-hoc discrete symmetry as such which can stabilize the DM. Rather we choose the $B - L$ charge (say n_{DM}) in such a way that there won't be any decay channel as displayed in Fig. 1 for the DM ϕ_{DM} [45]. For example, to avoid the cubic term in the scalar potential of the form $\phi_{\text{DM}}H_iH_j$ where H_i, H_j denote the physical masses for any of the scalars H, ϕ_1 or ϕ_8 , the possible values of $n_{\text{DM}} = 0, \pm 2, \pm 7, \pm 9, \pm 16$ are not allowed. Similarly if we don't want term like $\phi_{\text{DM}}H_iH_jH_k$, the value of n_{DM} is restricted to $n_{\text{DM}} \neq \pm 1, \pm 3, \pm 6, \pm 8, \pm 10$. Thus, the allowed values of n_{DM} are $\pm 4, \pm 5$ and fractional charges. The approach of ensuring stability of scalar DM particle with the model structure has been recently implemented in a $B - L$ model with right-handed neutrinos [17], while our model is one such variant with a modified scalar content and variety of exotic charges assigned to the additional fermion content of the $B - L$ model.

We choose $n_{\text{DM}} = 4$ to ensure the stability of the scalar singlet ϕ_{DM} and study its phenomenology in the prospects of dark matter observables such as relic abundance and direct detection cross section. Based on the structure of the model built, the DM can have scalar and gauge portal interactions. We proceed to study in detail the behaviour of DM

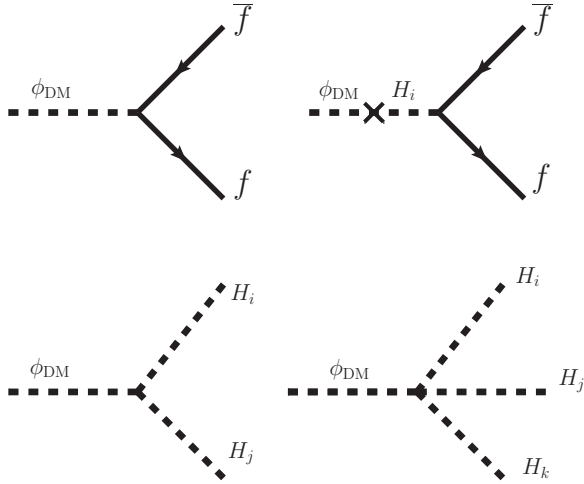


FIG. 1: Feynman diagrams leading to decay of scalar singlet dark matter ϕ_{DM} . The choice of $B - L$ charge to forbid these decay and stability of scalar singlet dark matter ϕ_{DM} is discussed in the text.

observables separately in dual portal scenario.

III. Z' PORTAL PHENOMENOLOGY

A. Relic abundance

The channels that contribute to relic density are shown in the left and middle panels of Fig. 2 and the expression for the corresponding annihilation cross sections are

$$\begin{aligned}
 \hat{\sigma}_{ff} &= \sum_f \frac{n_{\text{DM}}^2 (n_{\text{BL}}^f)^2 g_{\text{BL}}^4 c_f}{16\pi s} \frac{(s - 4M_{\text{DM}}^2)(s + 2M_f^2)}{[(s - M_{Z'}^2)^2 + M_{Z'}^2 \Gamma_{Z'}^2]} \frac{(s - 4M_f^2)^{\frac{1}{2}}}{(s - 4M_{\text{DM}}^2)^{\frac{1}{2}}}, \\
 \hat{\sigma}_{Z'H_i} &= \frac{n_{\text{DM}}^2 g_{\text{BL}}^6 (C_{H_i})^2}{16\pi s} \frac{(s - 4M_{\text{DM}}^2)}{[(s - M_{Z'}^2)^2 + M_{Z'}^2 \Gamma_{Z'}^2]} \left[1 + \frac{(s - (M_{Z'} + M_{H_i})^2)(s - (M_{Z'} - M_{H_i})^2)}{12sM_{Z'}^2} \right] \\
 &\quad \frac{\left[(s - (M_{Z'} + M_{H_i})^2)(s - (M_{Z'} - M_{H_i})^2) \right]^{\frac{1}{2}}}{[s(s - 4M_{\text{DM}}^2)]^{\frac{1}{2}}}, \tag{22}
 \end{aligned}$$

where $i = 1, 2, 3$ and

$$\begin{aligned}
 C_{H_1} &= 2\beta(64v_8 - v_1), \\
 C_{H_2} &= \sqrt{2}(64v_8 - v_1), \\
 C_{H_3} &= \sqrt{2}(64v_8 + v_1).
 \end{aligned}$$

The parameters c_f and n_{BL}^f denote the color charge and the $B - L$ charge of the fermion f with mass M_f . $M_{Z'}$ is the mass of the heavy gauge boson Z' given by $M_{Z'} = g_{\text{BL}} \sqrt{v_1^2 + 64v_8^2}$

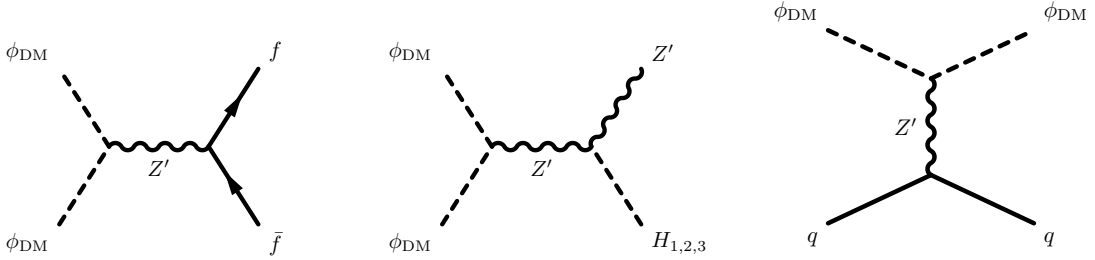


FIG. 2: Feynman diagrams for dark matter annihilation (left and middle) and scattering of DM from nucleon/quark (right panel) through Z' exchange. First two diagrams contribute to the relic density observable and the third one is appropriate in direct detection studies.

Parameters	n_{DM}	M_{H_2} [GeV]	M_{H_3} [GeV]	$v_{1,8}$ [GeV]	β
Values	4	1000	1500	2000	0.007

TABLE II: Fixed parameters for Z' -mediated DM observables.

with the decay width $\Gamma_{Z'}$. The relic abundance of dark matter is computed by

$$\Omega h^2 = \frac{2.14 \times 10^9 \text{ GeV}^{-1}}{g_*^{1/2} M_{\text{pl}}} \frac{1}{J(x_f)}, \quad (23)$$

where $M_{\text{pl}} = 1.22 \times 10^{19}$ GeV is the Planck mass, $g_* = 106.75$ denoting the total number of effective relativistic degrees of freedom, and $J(x_f)$ reads as

$$J(x_f) = \int_{x_f}^{\infty} \frac{\langle \sigma v \rangle(x)}{x^2} dx. \quad (24)$$

The thermally averaged annihilation cross section $\langle \sigma v \rangle$ is given by

$$\langle \sigma v \rangle(x) = \frac{x}{8M_{\text{DM}}^5 K_2^2(x)} \int_{4M_{\text{DM}}^2}^{\infty} \hat{\sigma} \times (s - 4M_{\text{DM}}^2) \sqrt{s} K_1 \left(\frac{x\sqrt{s}}{M_{\text{DM}}} \right) ds. \quad (25)$$

The functions K_1 , K_2 denote the modified Bessel functions and $x = M_{\text{DM}}/T$, where T is the temperature. The analytical expression for the freeze out parameter x_f is given as

$$x_f = \ln \left(\frac{0.038 g M_{\text{pl}} M_{\text{DM}} \langle \sigma v \rangle(x_f)}{(g_* x_f)^{1/2}} \right). \quad (26)$$

Here g is the count of number of degrees of freedom of the dark matter particle S . We have implemented the model in LanHEP [46] to produce the model files required for micrOMEGAs [47–49] package to compute the relic abundance of scalar DM. The parameters that are fixed during the analysis are shown in Table. II. The flexibility of gauge portal study is that, just two parameters are relevant i.e., g_{BL} and $M_{Z'}$. The value of n_{DM} not only stabilizes the DM particle but also scales the annihilation cross section thereby showing up in relic density. Fig. 3 displays the variation of DM abundance Ωh^2 with the singlet DM mass M_{DM} and the behavior with various parameters. All the curves in Fig. 3 reach the current relic density of PLANCK [1] near the resonance ($M_{\text{DM}} \simeq \frac{M_{Z'}}{2}$). The gauge coupling g_{BL} scales

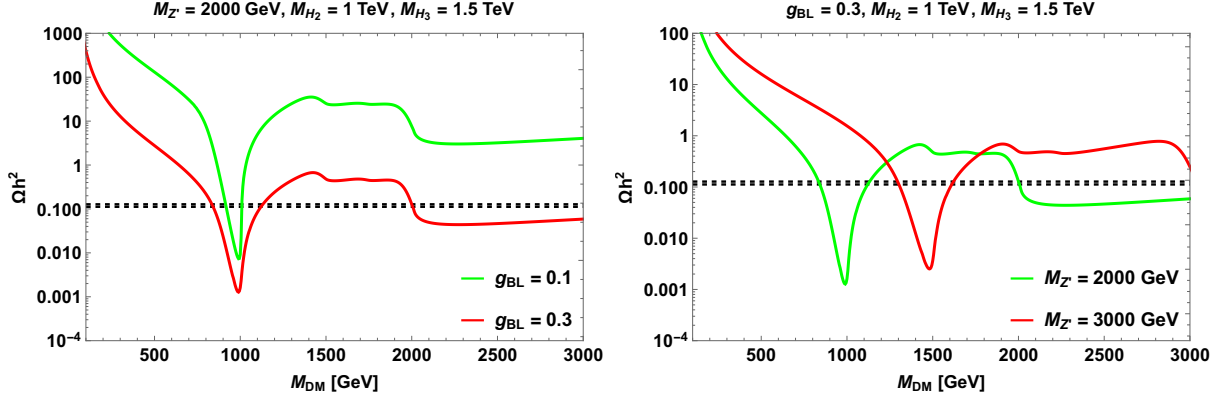


FIG. 3: Variation of relic abundance Ωh^2 with the mass of DM shown with two representative values of g_{BL} (left panel) and $M_{Z'}$ (right panel) for $n_{\text{DM}} = 4$. Here the horizontal dashed lines denote the 3σ range in current relic density [1].

the annihilation cross section i.e., lower couplings give lower annihilation cross section. The channels $SS \rightarrow f\bar{f}$ drive the relic density until the channels $SS \rightarrow Z'H_1$, $SS \rightarrow Z'H_2$ and $SS \rightarrow Z'H_3$ get kinematically allowed.

B. Direct searches

Now we look for the constraints on the model parameters due to direct detection limits. The interaction terms for Z' -mediated t-channel processes shown in the extreme right panel of Fig. 2 is given as

$$\mathcal{L} \supset -n_{\text{DM}} i g_{\text{BL}} Z'_\mu (S \partial^\mu A - A \partial^\mu S) - \frac{1}{3} g_{\text{BL}} Z'_\mu \bar{u} \gamma^\mu u - \frac{1}{3} g_{\text{BL}} Z'_\mu \bar{d} \gamma^\mu d. \quad (27)$$

Thus, the effective Lagrangian follows as

$$i\mathcal{L}_{\text{eff}} \supset -\frac{n_{\text{DM}} g_{\text{BL}}^2}{3M_{Z'}^2} (S \partial^\mu A - A \partial^\mu S) \bar{u} \gamma_\mu u - \frac{n_{\text{DM}} g_{\text{BL}}^2}{3M_{Z'}^2} (S \partial^\mu A - A \partial^\mu S) \bar{d} \gamma_\mu d. \quad (28)$$

The DM-nuclei cross-section of the singlet scalar DM mediated by the gauge boson Z' is given by [50–57]

$$\sigma_{\text{SI}}^{\text{N}} = \frac{1}{16\pi} \left(\frac{M_{\text{N}} M_{\text{DM}}}{M_{\text{N}} + M_{\text{DM}}} \right)^2 |b_{\text{N}}|^2, \quad (29)$$

where M_{N} is the nuclei mass and the coefficient b_{N} is given by

$$b_{\text{N}} = (A - Z)b_n + Zb_p, \quad b_n = b_u + 2b_d, \quad b_p = 2b_u + b_d, \quad (30)$$

Here Z and A denote the atomic and the mass number respectively. The parameters b_u and b_d of the effective Lagrangian are defined as

$$\mathcal{L}_{\text{eff}} = b_q X^\mu \bar{q} \gamma^\mu q, \quad \text{where } q = (u, d). \quad (31)$$

In the present model, X^μ takes the form of the vector current given by $X^\mu \simeq iS\partial^\mu A - iA\partial^\mu S$. Thus, one can find the value of $b_{p,n}$ as

$$b_p = b_n = i \frac{n_{\text{DM}} g_{\text{BL}}^2}{M_{Z'}^2}.$$

Therefore, b_N can have the value

$$b_N = iA \frac{n_{\text{DM}} g_{\text{BL}}^2}{M_{Z'}^2}.$$

Thus, the DM-nuclei SI contribution is given by

$$\sigma_{\text{SI}}^{\text{N}} = \frac{1}{16\pi} \left(\frac{M_{\text{N}} M_{\text{DM}}}{M_{\text{N}} + M_{\text{DM}}} \right)^2 |A|^2 \frac{n_{\text{DM}}^2 g_{\text{BL}}^4}{M_{Z'}^4}.$$

For single nucleon, the above expression becomes

$$\sigma_{Z'} = \frac{\mu^2}{16\pi} \frac{n_{\text{DM}}^2 g_{\text{BL}}^4}{M_{Z'}^4}. \quad (32)$$

where $\mu = \left(\frac{M_n M_{\text{DM}}}{M_n + M_{\text{DM}}} \right)$ is the reduced mass of DM-nucleon with M_n being the nucleon mass. We see that the $B - L$ charge n_{DM} remains as a scaling parameter in $\sigma_{Z'}$ alike relic density in Eqn. 22. It is convenient to write (in cm^2) as

$$\sigma_{Z'} = 7.75 \times 10^{-42} \left(\frac{\mu}{1 \text{ GeV}} \right)^2 \times n_{\text{DM}}^2 \times \left(\frac{1 \text{ TeV}}{\left(\frac{M_{Z'}}{g_{\text{BL}}} \right)} \right)^4. \quad (33)$$

We show in the left panel Fig. 4, the parameter space that satisfies the 3σ range in the current relic density limit [1] and the most stringent direct detection bound from XENON1T [58]. The right panel shows the WIMP-nucleon spin-independent cross section with the DM mass for the parameter space shown in the left panel.

C. Collider bounds

The $B - L$ models are further constrained by the collider limits. The extensive analysis of ATLAS and CMS collaborations in search of new heavy resonances in dilepton and dijet signals have derived a lower bound on the mass of Z' . Recent works [11, 16] have discussed the sensitivity of the bounds from ATLAS [60] on the parameters $M_{Z'}$ and g_{BL} in $B - L$ models. In the present work, we use CalcHEP [61, 62] to compute the production cross section of Z' . In the left panel of Fig. 5, we show the Z' production cross section times the branching ratio of dilepton ($ee, \mu\mu$) signal as a function of $M_{Z'}$. The black dashed line denotes the dilepton bound from ATLAS [60]. It is clear that the region below $M_{Z'} \simeq 3.7$ TeV is excluded for $g_{\text{BL}} = 0.4$. For $g_{\text{BL}} = 0.1$, $M_{Z'} < 2.3$ TeV is ruled out. We have $M_{Z'} \gtrsim 1.2$ TeV for $g_{\text{BL}} = 0.03$ and the mass region of $M_{Z'} \gtrsim 0.5$ TeV is allowed for $g_{\text{BL}} = 0.01$. The plot in the right panel of Fig. 5 shows the parameter space that satisfies 3σ range in the PLANCK relic density limit and the XENON1T constraint. The region to the right of both the dashed curves is consistent with LEP-II [63] and ATLAS [60] dilepton limit. We see that the ATLAS gives more stringent limit in the mass region $M_{Z'} \lesssim 2.7$ TeV.

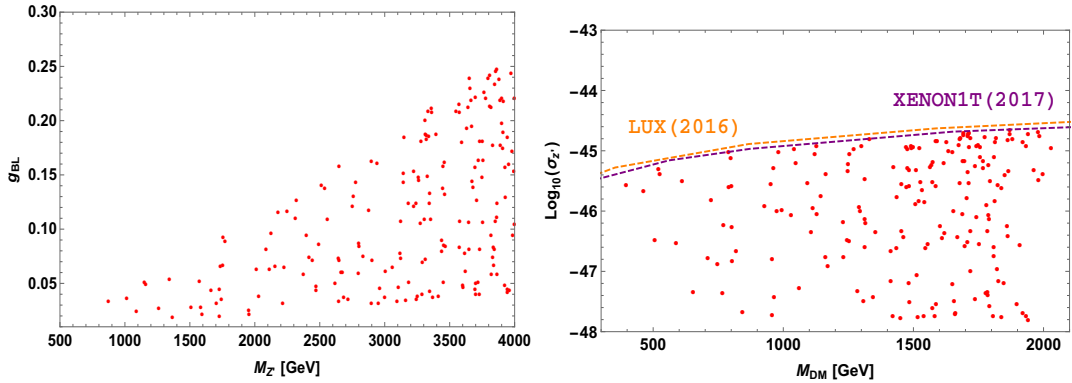


FIG. 4: Left panel denotes the parameters space in the plane of $(M_{Z'}, g_{BL})$ that satisfy the current relic density [1] in 3σ range and XENON1T [58]. The right panel depicts the WIMP-nucleon SI cross section with the mass of the scalar DM for the parameter space shown in the left panel. Here, the horizontal dashed lines denote the current bounds on spin-independent WIMP-nucleon cross section from the direct detection experiments LUX [59] and XENON1T [58].

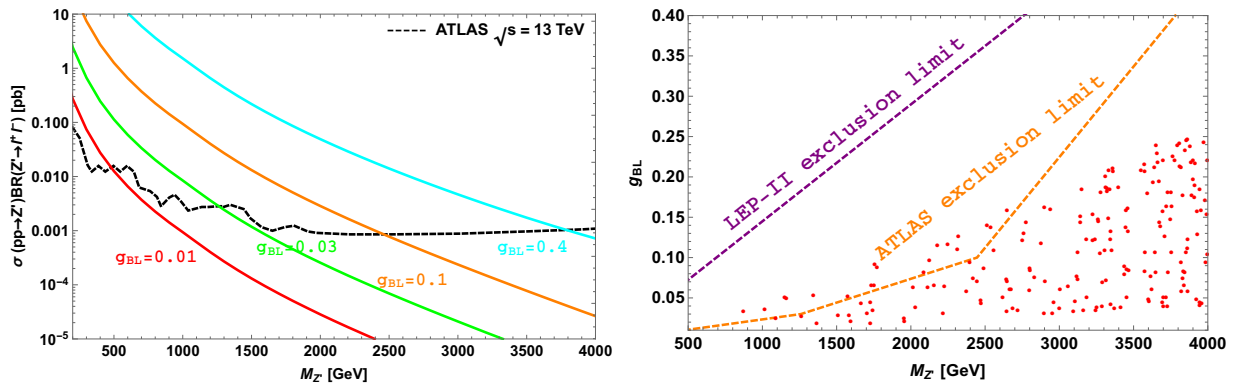


FIG. 5: Dilepton constraints from ATLAS on the current model are shown here. The black dashed line in the left panel represents the exclusion limit from ATLAS [60], with the colored lines being the dilepton signal cross sections for various values of g_{BL} as a function of $M_{Z'}$. The right panel shows exclusion limits from LEP-II and ATLAS exclusion limits in the plane of $M_{Z'}$ – g_{BL} . The red points are consistent with the 3σ range of the relic density limit of PLANCK and the direct detection limits from XENON1T.

D. Landau Pole

In the present work, we have extra neutral fermions with $B - L$ charges $-4, -4, +5$ required for consistent gauge anomaly free theory. Also there are scalars ϕ_1, ϕ_8 with $B - L$ charges $-1, +8$ and ϕ_{DM} with $n_{DM} = 4$. The presence of these additional field content with exotic $B - L$ charges can severely modify the running of the corresponding gauge coupling g_{BL} and can even lead to a Landau pole Λ_{LP} . Defining the $U(1)_{B-L}$ fine-structure coupling $\alpha_{BL} = \frac{g_{BL}^2}{4\pi}$, one finds the standard analytic one-loop solution for the renormalization-group

running from a scale λ to $\Lambda > \lambda$:

$$\frac{1}{\alpha_{\text{BL}}(\Lambda)} = \frac{1}{\alpha_{\text{BL}}(\lambda)} - \frac{b_{\text{BL}}}{2\pi} \log\left(\frac{\Lambda}{\lambda}\right). \quad (34)$$

The location of Landau pole Λ_{LP} can be obtained by $\alpha_{\text{BL}}^{-1}(\Lambda_{\text{LP}}) = 0$, given by the scale

$$\Lambda_{\text{LP}} \simeq \lambda \exp\left[\frac{2\pi}{b_{\text{BL}}} \alpha_{\text{BL}}^{-1}(\lambda)\right], \quad (35)$$

for $b_{\text{BL}} > 0$. We consider the $B - L$ breaking scale (λ) and all new particle masses at 10 TeV. The one-loop beta coefficient, b_{BL} can be computed using the standard formula

$$b_{\text{BL}} = -\frac{11}{3}C_2(G) + C_{\text{norm}}^2 \left[\frac{2}{3} \sum_{R_f} \left(\frac{n_{\text{BL}}^f}{2}\right)^2 \prod_{j \neq \text{BL}} d_j(R_f) + \frac{1}{3} \sum_{R_s} \left(\frac{n_{\text{BL}}^s}{2}\right)^2 \prod_{j \neq \text{BL}} d_j(R_s) \right]. \quad (36)$$

Here $n_{\text{BL}}^{f(s)}$ stands for the $B - L$ charge of the fermion (scalar). $C_2(G)$ denotes the quadratic Casimir operator for gauge bosons which takes the value N for $SU(N)$ and 0 if $U(1)$, $d_j(R_{f,s})$ indicate the dimension of representation $R_{f,s}$ under all the $SU(N)$ groups. Since the model can't be embedded in $SO(10)$ framework, the normalization factor C_{norm} is a free parameter. For instance, choosing $g_{\text{BL}} = 0.4$, the Landau pole is at

$$\Lambda_{\text{LP}} = \begin{cases} 5.72 \times 10^{11} \text{ GeV} & \text{if } C_{\text{norm}} = \sqrt{\frac{3}{2}}, \\ 2.48 \times 10^{23} \text{ GeV} & \text{if } C_{\text{norm}} = \sqrt{\frac{3}{5}}, \\ 1.07 \times 10^{35} \text{ GeV} & \text{if } C_{\text{norm}} = \sqrt{\frac{3}{8}}. \end{cases} \quad (37)$$

Thus, choosing suitable normalization factor, one can avoid the Landau pole below Planck scale.

IV. SCALAR PORTAL PHENOMENOLOGY

A. Relic density

With $n_{\text{DM}} = 4$, one can write a non-trivial term to the scalar potential as

$$\frac{\mu_{\text{D8}}}{2} \left[(\phi_{\text{DM}})^2 \phi_8^\dagger + (\phi_{\text{DM}}^\dagger)^2 \phi_8 \right]. \quad (38)$$

The masses of real and imaginary components of ϕ_{DM} are given by

$$\begin{aligned} M_S^2 &= \mu_{\text{DM}}^2 + \frac{\lambda_{\text{HD}}}{2} v^2 + \frac{\lambda_{\text{D1}}}{2} v_1^2 + \frac{\lambda_{\text{D8}}}{2} v_8^2 + \frac{\mu_{\text{D8}} v_8}{\sqrt{2}}, \\ M_A^2 &= \mu_{\text{DM}}^2 + \frac{\lambda_{\text{HD}}}{2} v^2 + \frac{\lambda_{\text{D1}}}{2} v_1^2 + \frac{\lambda_{\text{D8}}}{2} v_8^2 - \frac{\mu_{\text{D8}} v_8}{\sqrt{2}}. \end{aligned} \quad (39)$$

For simplicity, we consider $\lambda_{\text{HD}} = \lambda_{\text{H1}} = \lambda_{\text{H8}} = \lambda_{\text{D}}$. The expressions for annihilation cross

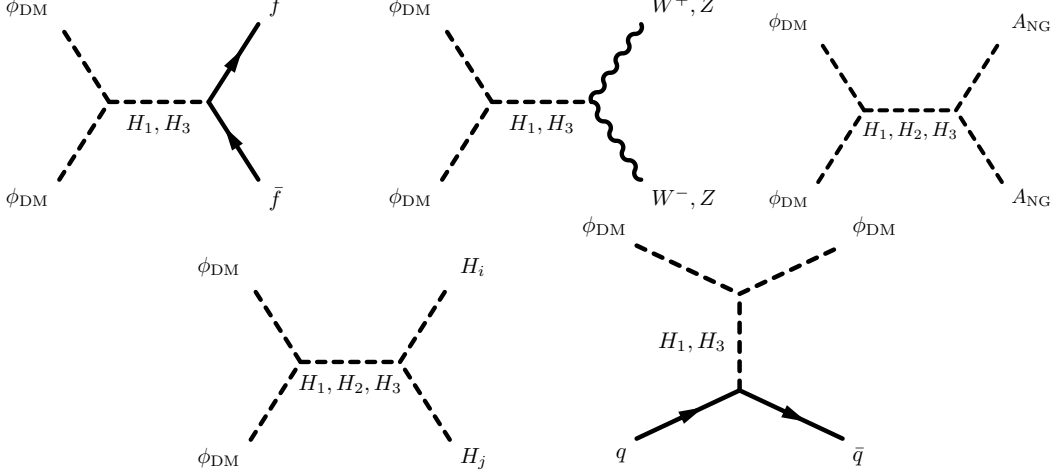


FIG. 6: Feynman diagrams contributing to relic density in the scalar portal case except the figure of t-channel process is relevant in direct detection studies.

section of various channels that contribute to relic density shown in Fig. 6 are

$$\hat{\sigma}_{ff}^S = \frac{1}{8\pi v^2 s} |F_1|^2 \sum_f M_f^2 c_f \frac{(s - 4M_f^2)^{\frac{3}{2}}}{(s - 4M_{\text{DM}}^2)^{\frac{1}{2}}}, \quad (40)$$

$$\hat{\sigma}_{WW}^S = \frac{s}{16\pi v^2} |F_1|^2 \left(1 - \frac{4M_W^2}{s} + \frac{12M_W^4}{s^2}\right) \frac{(s - 4M_W^2)^{\frac{1}{2}}}{(s - 4M_{\text{DM}}^2)^{\frac{1}{2}}}, \quad (41)$$

$$\hat{\sigma}_{ZZ}^S = \frac{s}{32\pi v^2} |F_1|^2 \left(1 - \frac{4M_Z^2}{s} + \frac{12M_Z^4}{s^2}\right) \frac{(s - 4M_Z^2)^{\frac{1}{2}}}{(s - 4M_{\text{DM}}^2)^{\frac{1}{2}}}, \quad (42)$$

$$\hat{\sigma}_{\text{NG}}^S = \frac{1}{8\pi} \left(\frac{1}{v_1 v_8 (v_1^2 + 64v_8^2)}\right)^2 |F_2|^2 \frac{s^{\frac{3}{2}}}{(s - 4M_{\text{DM}}^2)^{\frac{1}{2}}}, \quad (43)$$

where

$$F_1 = \frac{\lambda_{\text{DH1}}}{[(s - M_{H_1}^2) + iM_{H_1}\Gamma_{H_1}]} - \frac{\sqrt{2}\beta\lambda_{\text{DH3}}}{[(s - M_{H_3}^2) + iM_{H_3}\Gamma_{H_3}]},$$

$$F_2 = -\frac{\lambda_{\text{DH1}}\beta(v_1^3 + 64v_8^3)}{[(s - M_{H_1}^2) + iM_{H_1}\Gamma_{H_1}]} + \frac{\lambda_{\text{DH2}}(v_1^3 - 64v_8^3)}{\sqrt{2}[(s - M_{H_2}^2) + iM_{H_2}\Gamma_{H_2}]} - \frac{\lambda_{\text{DH3}}(v_1^3 + 64v_8^3)}{\sqrt{2}[(s - M_{H_3}^2) + iM_{H_3}\Gamma_{H_3}]},$$

with c_f and M_f denoting the color charge and mass of the the SM fermion f respectively. Finally, for the Higgs sector annihilation channels we have

$$\hat{\sigma}_{H_i H_j}^S = \frac{1}{16\pi s n!} |F_{ij}|^2 \frac{[(s - (M_{H_i} + M_{H_j})^2)(s - (M_{H_i} - M_{H_j})^2)]^{\frac{1}{2}}}{[s(s - 4M_{\text{DM}}^2)]^{\frac{1}{2}}},$$

where

$$F_{ij} = (1 + 2\beta^2)\lambda_{\text{D}}\delta_{ij} + \frac{\lambda_{\text{DH1}}\lambda_{1ij}}{[(s - M_{H_1}^2) + iM_{H_1}\Gamma_{H_1}]} + \frac{\lambda_{\text{DH2}}\lambda_{2ij}}{[(s - M_{H_2}^2) + iM_{H_2}\Gamma_{H_2}]} + \frac{\lambda_{\text{DH3}}\lambda_{3ij}}{[(s - M_{H_3}^2) + iM_{H_3}\Gamma_{H_3}]},$$

Coupling	Expression [GeV]
λ_{DH1}	$v\lambda_{\text{D}} - \frac{1}{4}\beta(8v_1\lambda_{\text{D}} - \sqrt{2}\mu_{\text{D8}})$
λ_{DH2}	$-\frac{\mu_{\text{D8}}}{4}$
λ_{DH3}	$-\sqrt{2}v_1\lambda_{\text{D}} - \sqrt{2}v\beta\lambda_{\text{D}} + \frac{\mu_{\text{D8}}}{4}$

TABLE III: Dark matter couplings to scalars.

In all the above expressions $i, j = 1, 2, 3$, and $\lambda_{\text{DH}i}$ denote the coupling of the terms $A^2 H_i$. We show in Fig. 7, the scalar portal relic abundance as a function of DM mass. The PLANCK limit on relic density is met near the resonance of three scalar propagators. The channels with $H_1 H_1$ and $A_{\text{NG}} A_{\text{NG}}$ in final state can only give resonance near $M_{\text{DM}} \simeq \frac{M_{H_2}}{2}$. However, the coupling λ_{211} vanishes. Hence, the channel with NG pair plays a crucial role in giving the resonance in H_2 propagator for non-zero λ_{DH2} ($= \mu_{\text{D8}}$) given in Table. III. One can also notice that the coupling μ_{D8} induces mass splitting in the scalar components given in Eqn. 39, which is essential to generate light neutrino mass at one loop level to be discussed in the upcoming section.

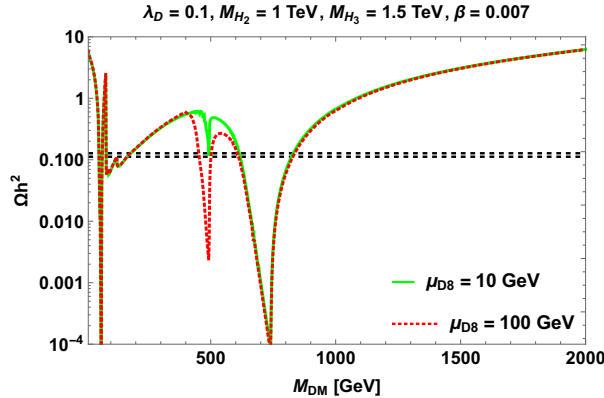


FIG. 7: Variation of relic abundance Ωh^2 with the mass of DM for various values of μ_{D8} parameter. Here the horizontal dashed lines denote the 3σ range in current relic density [1].

B. Direct searches

In the scalar portal scenario, the DM-WIMP nucleon cross section is given by

$$\sigma_S = \frac{\mu^2 M_n^2}{4\pi v^2 M_{\text{DM}}^2} \left[\frac{\lambda_{\text{DH1}}}{M_{H_1}^2} - \frac{\sqrt{2}\lambda_{\text{DH3}}\beta}{M_{H_3}^2} \right]^2 f_p^2, \quad (44)$$

where M_n is the nucleon mass, μ denotes the reduced mass of WIMP-nucleon system and f_p is given by

$$f_p = \frac{2}{9} + \frac{7}{9} \sum_{q=u,d,s} f_{Tq}^p. \quad (45)$$

Typical values for proton are $f_{Tu}^p = 0.020 \pm 0.004$, $f_{Td}^p = 0.026 \pm 0.005$ and $f_{Ts}^p = 0.118 \pm 0.062$ [64]. Varying the model parameters given in Table. IV, Fig. 8 left panel denotes the parameter space in $M_{H_3} - M_{DM}$ plane satisfying 3σ range on current relic density limit by PLANCK and the right panel denotes the allowed parameter space (corresponding to the allowed parameters of the left panel), consistent with XENON1T limit. We see that the data points near the resonance of SM Higgs H_1 doesn't satisfy the XENON1T limit on WIMP-nucleon cross section.

Parameters	Range
μ_{D8} [GeV]	10 – 100
λ_D	0.001 – 0.1
$v_{1,8}$ [GeV]	2000
M_{H_2} [GeV]	1000, 2000
M_{H_3} [GeV]	$M_{H_2} - 4000$
M_{DM} [GeV]	20 – 2000
β	0.001 – 0.016

TABLE IV: Parameters and their ranges for scalar portal analysis.

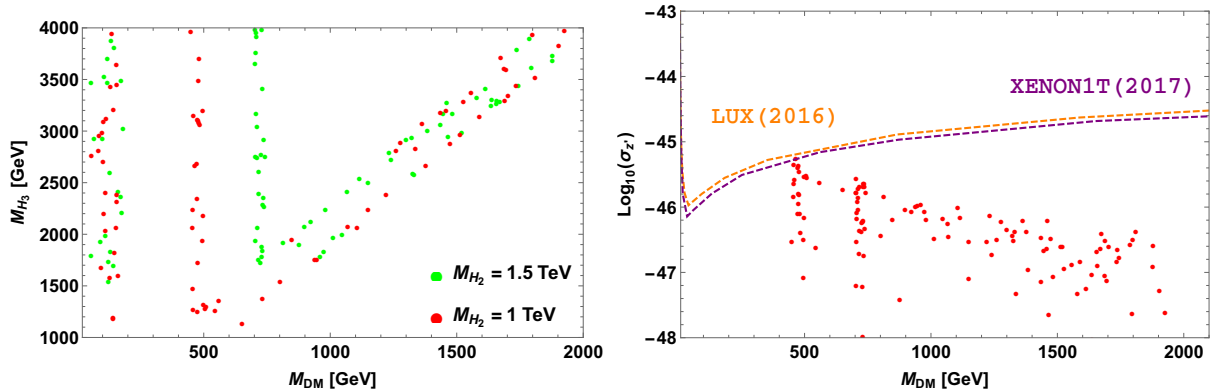


FIG. 8: Region of $M_{DM} - M_{H_3}$ that meets the 3σ range on current relic density limit of PLANCK in left panel. Right panel denotes the parameter space taken from left panel that satisfies the XENON1T limit as well. Dashed lines denote the upper limit on WIMP-nucleon cross section by LUX [59] and XENON1T [58].

Sl. No.	μ_{D8}	$\sqrt{ Y_{i\alpha_1} Y_{j\alpha_1} }$	M_{DM} [GeV]	Λ [TeV]	m_ν [GeV]	Ωh^2	$\text{Log}_{10}\sigma_S$ [cm^2]
1.	96.8	0.026	448	50	4.01×10^{-11}	0.1154	-46.517
2.	21.3	0.056	483	50	4.09×10^{-11}	0.123	-46.376
3.	21.3	0.22	483	100	3.95×10^{-11}	0.123	-46.376

TABLE V: Sample benchmark for radiative ν -mass.

V. LIGHT NEUTRINO MASS

The light neutrino mass in this model can be achieved by radiative mechanism. The model structure permits us to write a dim-6 Yukawa interaction term of the form¹

$$\frac{1}{\Lambda^2} \sum_{\alpha=1,2} Y_{i\alpha} \overline{(\ell_L)_i} \tilde{H} N_{\alpha R} \phi_{DM} \phi_1. \quad (46)$$

Now, it is possible to generate the light neutrino mass at one loop level as shown in Fig. 9. If we assume the masses of real and imaginary components of ϕ_{DM} satisfy the relation $(M_S^2 + M_A^2)/2 \gg M_S^2 - M_A^2 = \sqrt{2}\mu_{D8}v_8$, the expression for the radiatively generated neutrino mass is [43]

$$(\mathcal{M}_\nu)_{ij} = \frac{\sqrt{2}\mu_{D8}v_8v_1^2v_2^2}{16\pi^2\Lambda^4} \sum_{\alpha=1}^3 \frac{Y_{i\alpha}Y_{j\alpha}M_{D\alpha}}{m_0^2 - M_{D\alpha}^2} \left[1 - \frac{M_{D\alpha}^2}{m_0^2 - M_{D\alpha}^2} \ln \frac{m_0^2}{M_{D\alpha}^2} \right], \quad (47)$$

where we denote $m_0^2 = (M_S^2 + M_A^2)/2$. If $M_{D\alpha}^2 \gg m_0^2$, then

$$(\mathcal{M}_\nu)_{ij} = \frac{\sqrt{2}\mu_{D8}v_8v_1^2v_2^2}{16\pi^2\Lambda^4} \sum_{\alpha=1}^3 \frac{Y_{i\alpha}Y_{j\alpha}}{M_{D\alpha}} \left[\ln \frac{M_{D\alpha}^2}{m_0^2} - 1 \right]. \quad (48)$$

Here $M_{D\alpha} = (U^T M U)_\alpha$ and $N_{D\alpha} = U_{\alpha\beta}^\dagger N_\beta$, with M being the Majorana mass matrix. Assuming the lightest exotic fermion gives dominant contribution to the light neutrino mass matrix and considering $(v_1, v_8, M_{D\alpha_1}) \sim (2, 2, 3)$ TeV ($M_{D\alpha_1}$ being the mass of the lightest exotic fermion mass eigenstate), we show sample benchmark values in Table. V that satisfy PLANCK, XENON1T limit and ν -mass simultaneously. We conclude that this model is quite advantageous to explain the light neutrino mass even without the small Yukawa couplings.

VI. SEMI-ANNIHILATIONS FOR SCALAR DARK MATTER

Fractional $B - L$ charge to the inert scalar can induce semi-annihilations which can show up in dark matter relic abundance (see Refs.[17, 67]). For instance when $n_{DM} = 1/3$, there is a quartic term in the Lagrangian of the form

$$\mathcal{L}_{1/3} = \frac{\lambda'_{DM}}{3} \phi_{DM}^3 \phi_1 + \text{h.c.} \quad (49)$$

¹ The interaction term in Eqn. 46 can induce the decay $\nu_i \rightarrow \nu_j + A_{NG}$. However the decay rate of this channel can be greater than the age of the universe [65]. The effect of neutrino decay in neutrino oscillations has been investigated in literature [66]. However, this study is beyond the scope of our work.

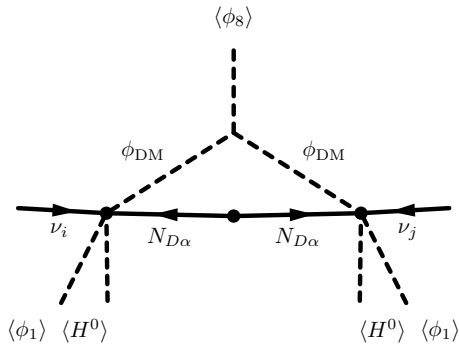


FIG. 9: Radiative generation of neutrino mass

With the Feynman diagram shown in Fig. 10, the cross section of all possible semi-annihilation channels are

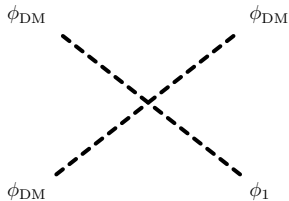


FIG. 10: Feynman diagram for the semi-annihilation vertex.

$$\begin{aligned}
\hat{\sigma}_{H_1}^{1/3} &= \frac{\lambda'_{\text{DM}}{}^2 \beta^2 [(s - (M_{\text{DM}} + M_{H_1})^2)(s - (M_{\text{DM}} - M_{H_1})^2)]^{\frac{1}{2}}}{64\pi s [s(s - 4M_{\text{DM}}^2)]^{\frac{1}{2}}}, \\
\hat{\sigma}_{H_2}^{1/3} &= \frac{\lambda'_{\text{DM}}{}^2 [(s - (M_{\text{DM}} + M_{H_2})^2)(s - (M_{\text{DM}} - M_{H_2})^2)]^{\frac{1}{2}}}{128\pi s [s(s - 4M_{\text{DM}}^2)]^{\frac{1}{2}}}, \\
\hat{\sigma}_{H_3}^{1/3} &= \frac{\lambda'_{\text{DM}}{}^2 [(s - (M_{\text{DM}} + M_{H_3})^2)(s - (M_{\text{DM}} - M_{H_3})^2)]^{\frac{1}{2}}}{128\pi s [s(s - 4M_{\text{DM}}^2)]^{\frac{1}{2}}}.
\end{aligned} \tag{50}$$

We display in Fig. 11 the effect of semi-annihilation channel on the relic abundance observable. Resonance near $M_{\text{DM}} \simeq \frac{M_{H_2}}{2}$ is not achieved as the term in Eqn. 38 doesn't exist for $n_{\text{DM}} = 1/3$, in turn making λ_{DH_2} to be zero. These new channels begin to pop up once mass of DM is above the mass of the physical scalar appearing in the final state. We see that the channel with H_2 and H_3 as one of the final state particles have a significant effect while the Higgs channel attains a β^2 suppression. This scenario is very appealing as the dark matter phenomenology is determined by three free parameters i.e, λ'_{DM} , M_{DM} and the mass of the physical scalar. Similarly, one can also perform the same analysis for $n_{\text{DM}} = 8/3$ as well.

VII. COMMENT ON INDIRECT SIGNALS

No indirect signals are expected in Z' -portal scenario as the annihilation rate today is velocity suppressed [17]. Moving to the scalar-portal, we briefly comment as follows.

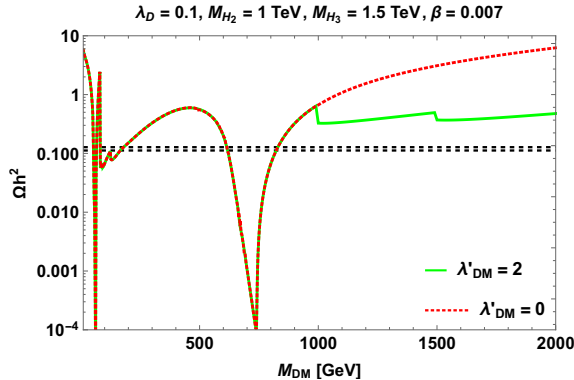


FIG. 11: Relic abundance Ωh^2 with the mass of DM plotted for two values of λ'_{DM} with the choice of $n_{\text{DM}} = 1/3$.

A. Gamma ray excess

Fermi-LAT report of excess in γ -ray emission, appearing as a peak around 1 – 3 GeV energy range [68, 69] can be well fitted by a DM maximally annihilating to $b\bar{b}$ channel with the mass range 35 – 165 GeV and $\langle\sigma v\rangle = (1 - 3) \times 10^{-26} \text{ cm}^3\text{s}^{-1}$ [70]. In the current model, the only way that to explain this excess is near the Higgs resonance where the relic density is met near $M_{\text{DM}} \simeq \frac{M_{H_1}}{2}$. However, from Fig. 8, the data points satisfying PLANCK limit (near Higgs resonance) in the left panel are eliminated by the direct detection bounds of XENON1T and LUX, conveyed in the right panel. Hence, the present model does not accommodate the excess γ -ray emission of Fermi-LAT.

B. Positron excess

The excess in positron signal reported by PAMELA [71] and AMS-02 [72] can be well explained by a DM with mass 350 and 894 GeV annihilating to $(e^+e^- \text{ or } \mu^+\mu^-)$ and $\tau^+\tau^-$ respectively. Another possibility is with a two scalar final state channel that subsequently decays to charged lepton pairs for the DM masses 350 and 590 GeV [73]. However, at all these mass values of DM, the channel with W-boson pair maximally contributes to the scalar-portal relic density. Therefore, we don't get a proper fit to the observed excess in this model dependent framework.

VIII. CONCLUSION

In this article, we have presented in detail the scalar dark matter phenomenology in the context of an anomaly free $U(1)_{B-L}$ extension of SM. A possible solution to cancel out the resulting non-trivial triangle anomalies of the gauge extension, three heavy neutral fermions N_{iR} ($i = 1, 2, 3$) with $B - L$ charges $-4, -4$ and $+5$ are added to the existing lepton content of the standard model. Furthermore, the scalar sector is enriched with two scalar singlets ϕ_1 and ϕ_8 to spontaneously break the $U(1)_{B-L}$ gauge symmetry and also to provide the

Majorana mass terms for the newly added fermions N_{iR} . A scalar singlet ϕ_{DM} is introduced such that the $U(1)_{B-L}$ symmetry takes the burden to forbid its decay making it a stable dark matter candidate. Three physical scalars and a heavy gauge boson Z' , a resultant of having $U(1)_{B-L}$ as local gauge symmetry act as mediators between the visible and dark sector.

We have studied the scalar spectrum emphasizing the minimization conditions, vacuum stability, perturbative unitarity conditions and their acquired masses after spontaneous symmetry breaking of $SU(2)_L \times U(1)_Y \times U(1)_{B-L}$ gauge symmetry. Choosing a particular $B - L$ charge that can stabilize ϕ_{DM} , we have investigated thoroughly the relic density and of scalar singlet dark matter in the Z' and scalar-portal scenarios. Applying the limits on relic density by PLANCK and the most stringent bounds on WIMP-nucleon spin-independent cross section by LUX and XENON1T, we have obtained the consistent parameter space. In collider studies, we have used ATLAS dilepton limits on the gauge coupling g_{BL} and the mass of the new vector boson $M_{Z'}$. We found that there is enough region for the model parameters to meet all the experimental bounds.

This remarkable gauge extension is economical in particle content and rich in phenomenology. A unique feature of this model is that a massless physical Goldstone boson, which plays a key role in scalar-portal relic density. We have discussed the mechanism to obtain the light neutrino mass at one-loop level, with the dark matter singlet running in the loop, and a suitable benchmark, where the dark matter observables and light neutrino mass are simultaneously consistent. We have included discussions regarding semi-annihilations of dark matter and its imprint on relic density for a choice of fractional $B - L$ charge for the scalar dark matter. We finally commented on indirect signals in the present model. To conclude, the explored model is quite consistent with current bounds of recent and ongoing dark matter experiments and a testable framework built based on the well-tested local gauge principles of Standard Model.

ACKNOWLEDGMENT

SS would like to thank Dr. Soumya Rao for the help in micrOMEGAs code and Department of Science and Technology (DST) - Inspire Fellowship division, Govt of India for the financial support through ID No. IF130927. RM would like to thank Science and Engineering Research Board (SERB), Government of India for financial support through grant No. SB/S2/HEP-017/2013. SP would like to acknowledge the warm hospitality provided by University of Hyderabad, India, between 22nd – 29th March, 2017, during which this work was completed.

Appendix A: Massless Goldstone interaction terms

1. Exotic fermion sector

The massless mode, A_{NG} can couple to the heavy fermions by the Majorana mass term in eqn. 6 as

$$\frac{iA_{\text{NG}}}{\sqrt{v_1^2 + 64v_8^2}} \left[\sum_{\alpha=1,2} \frac{8v_8 h_{\alpha 3}}{\sqrt{2}} \overline{N_{\alpha R}^c} N_{3R} + \sum_{\alpha,\beta=1,2} \frac{v_1 h_{\alpha\beta}}{\sqrt{2}} \overline{N_{\alpha R}^c} N_{\beta R} \right], \quad (\text{A1})$$

where the Majorana mass matrix takes the form

$$M = \begin{pmatrix} h_{11}\langle\phi_8\rangle & h_{12}\langle\phi_8\rangle & h_{13}\langle\phi_1\rangle \\ h_{12}\langle\phi_8\rangle & h_{22}\langle\phi_8\rangle & h_{23}\langle\phi_1\rangle \\ h_{13}\langle\phi_1\rangle & h_{23}\langle\phi_1\rangle & 0 \end{pmatrix}. \quad (\text{A2})$$

Writing it in a simplified form as

$$M = \begin{pmatrix} x & a & b \\ a & x & b \\ b & b & 0 \end{pmatrix}, \quad (\text{A3})$$

which can be obtained assuming the Yukawa couplings to satisfy the relation $h_{11} \approx h_{22}$ and $y_{13} \approx y_{23}$ along with $v_1 \approx v_8$. The mass matrix can be diagonalized by using normalized eigenvector matrix as $M_{D\alpha} = (U^T M U)_\alpha$, and the mass eigenstates are given as $N_{D\alpha} = U_{\alpha\beta}^\dagger N_\beta$.

2. Scalar sector

The coupling of A_{NG} to the new scalar fields is given as

$$\frac{2}{v_1 v_8 (v_1^2 + 64v_8^2)} (\partial_\mu A_{\text{NG}})^2 \left[-H_1 \beta (v_1^3 + 64v_8^3) + \frac{H_2}{\sqrt{2}} (v_1^3 - 64v_8^3) - \frac{H_3}{\sqrt{2}} (v_1^3 + 64v_8^3) \right]. \quad (\text{A4})$$

-
- [1] **Planck**, P. A. R. Ade *et al.*, “*Planck 2015 results. XIII. Cosmological parameters*,” *Astron. Astrophys.* **594** (2016) A13, [arXiv:1502.01589](#).
- [2] G. Arcadi, M. Dutra, P. Ghosh, M. Lindner, Y. Mambrini, M. Pierre, S. Profumo, and F. S. Queiroz, “*The Waning of the WIMP? A Review of Models, Searches, and Constraints*,” [arXiv:1703.07364](#).
- [3] E. E. Jenkins, “*Searching for a (B – L) Gauge Boson in p̄p Collisions*,” *Phys. Lett.* **B192** (1987) 219–222.
- [4] W. Buchmuller, C. Greub, and P. Minkowski, “*Neutrino masses, neutral vector bosons and the scale of B-L breaking*,” *Phys. Lett.* **B267** (1991) 395–399.

- [5] L. Basso, A. Belyaev, S. Moretti, and C. H. Shepherd-Themistocleous, “*Phenomenology of the minimal B-L extension of the Standard model: Z' and neutrinos,*” *Phys. Rev.* **D80** (2009) 055030, [arXiv:0812.4313](#).
- [6] W. Emam and S. Khalil, “*Higgs and Z-prime phenomenology in B-L extension of the standard model at LHC,*” *Eur. Phys. J.* **C52** (2007) 625–633, [arXiv:0704.1395](#).
- [7] S. Khalil, “*Low scale B - L extension of the Standard Model at the LHC,*” *J. Phys.* **G35** (2008) 055001, [arXiv:hep-ph/0611205](#).
- [8] S. Iso, N. Okada, and Y. Orikasa, “*Classically conformal B - L extended Standard Model,*” *Phys. Lett.* **B676** (2009) 81–87, [arXiv:0902.4050](#).
- [9] S. Kanemura, T. Matsui, and H. Sugiyama, “*Neutrino mass and dark matter from gauged U(1)_{B-L} breaking,*” *Phys. Rev.* **D90** (2014) 013001, [arXiv:1405.1935](#).
- [10] M. Lindner, D. Schmidt, and T. Schwetz, “*Dark Matter and neutrino masses from global U(1)_{BL} symmetry breaking,*” *Phys. Lett.* **B705** (2011) 324–330, [arXiv:1105.4626](#).
- [11] N. Okada and S. Okada, “*Z'_{BL} portal dark matter and LHC Run-2 results,*” *Phys. Rev.* **D93** (2016) no. 7, 075003, [arXiv:1601.07526](#).
- [12] N. Okada and S. Okada, “*Z'-portal right-handed neutrino dark matter in the minimal U(1)_X extended Standard Model,*” *Phys. Rev.* **D95** (2017) no. 3, 035025, [arXiv:1611.02672](#).
- [13] S. Bhattacharya, S. Jana, and S. Nandi, “*Neutrino Masses and Scalar Singlet Dark Matter,*” *Phys. Rev.* **D95** (2017) no. 5, 055003, [arXiv:1609.03274](#).
- [14] A. Biswas, S. Choubey, and S. Khan, “*Galactic gamma ray excess and dark matter phenomenology in a U(1)_{B-L} model,*” *JHEP* **08** (2016) 114, [arXiv:1604.06566](#).
- [15] W. Wang and Z.-L. Han, “*Radiative linear seesaw model, dark matter, and U(1)_{B-L},*” *Phys. Rev.* **D92** (2015) 095001, [arXiv:1508.00706](#).
- [16] M. Klasen, F. Lyonnet, and F. S. Queiroz, “*NLO+NLL Collider Bounds, Dirac Fermion and Scalar Dark Matter in the B-L Model,*” [arXiv:1607.06468](#).
- [17] W. Rodejohann and C. E. Yaguna, “*Scalar dark matter in the B-L model,*” *JCAP* **1512** (2015) no. 12, 032, [arXiv:1509.04036](#).
- [18] M. Lindner, D. Schmidt, and A. Watanabe, “*Dark matter and U(1)' symmetry for the right-handed neutrinos,*” *Phys. Rev.* **D89** (2014) no. 1, 013007, [arXiv:1310.6582](#).
- [19] N. Okada and O. Seto, “*Higgs portal dark matter in the minimal gauged U(1)_{B-L} model,*” *Phys. Rev.* **D82** (2010) 023507, [arXiv:1002.2525](#).
- [20] N. Okada and Y. Orikasa, “*Dark matter in the classically conformal B-L model,*” *Phys. Rev.* **D85** (2012) 115006, [arXiv:1202.1405](#).
- [21] T. Basak and T. Mondal, “*Constraining Minimal U(1)_{B-L} model from Dark Matter Observations,*” *Phys. Rev.* **D89** (2014) 063527, [arXiv:1308.0023](#).
- [22] B. L. Sanchez-Vega, J. C. Montero, and E. R. Schmitz, “*Complex Scalar DM in a B-L Model,*” *Phys. Rev.* **D90** (2014) no. 5, 055022, [arXiv:1404.5973](#).
- [23] M. Duerr, P. Fileviez Perez, and J. Smirnov, “*Simplified Dirac Dark Matter Models and Gamma-Ray Lines,*” *Phys. Rev.* **D92** (2015) no. 8, 083521, [arXiv:1506.05107](#).
- [24] J. Guo, Z. Kang, P. Ko, and Y. Orikasa, “*Accidental dark matter: Case in the scale invariant local B-L model,*” *Phys. Rev.* **D91** (2015) no. 11, 115017, [arXiv:1502.00508](#).

- [25] A. Dasgupta, C. Hati, S. Patra, and U. Sarkar, “*A minimal model of TeV scale WIMP_y leptogenesis,*” [arXiv:1605.01292](#).
- [26] T. Modak, S. Sadhukhan, and R. Srivastava, “*750 GeV diphoton excess from gauged BL symmetry,*” *Phys. Lett.* **B756** (2016) 405–412, [arXiv:1601.00836](#).
- [27] E. Ma and R. Srivastava, “*Dirac or inverse seesaw neutrino masses with B – L gauge symmetry and S₃ flavor symmetry,*” *Phys. Lett.* **B741** (2015) 217–222, [arXiv:1411.5042](#).
- [28] E. Ma and R. Srivastava, “*Dirac or inverse seesaw neutrino masses from gauged B – L symmetry,*” *Mod. Phys. Lett.* **A30** (2015) no. 26, 1530020, [arXiv:1504.00111](#).
- [29] E. Ma, N. Pollard, R. Srivastava, and M. Zakeri, “*Gauge B – L Model with Residual Z₃ Symmetry,*” *Phys. Lett.* **B750** (2015) 135–138, [arXiv:1507.03943](#).
- [30] S. Patra, W. Rodejohann, and C. E. Yaguna, “*A new B-L model without right-handed neutrinos,*” *JHEP* **09** (2016) 076, [arXiv:1607.04029](#).
- [31] P. Minkowski, “ *$\mu \rightarrow e\gamma$ at a Rate of One Out of 10⁹ Muon Decays?,*” *Phys. Lett.* **B67** (1977) 421–428.
- [32] R. N. Mohapatra and G. Senjanovic, “*Neutrino Mass and Spontaneous Parity Violation,*” *Phys. Rev. Lett.* **44** (1980) 912.
- [33] J. Schechter and J. W. F. Valle, “*Neutrino Masses in SU(2) x U(1) Theories,*” *Phys. Rev.* **D22** (1980) 2227.
- [34] M. Gell-Mann, P. Ramond, and R. Slansky, “*Complex Spinors and Unified Theories,*” *Conf. Proc.* **C790927** (1979) 315–321, [arXiv:1306.4669](#).
- [35] J. C. Montero and V. Pleitez, “*Gauging U(1) symmetries and the number of right-handed neutrinos,*” *Phys. Lett.* **B675** (2009) 64–68, [arXiv:0706.0473](#).
- [36] S. Singirala, R. Mohanta, S. Patra, and S. Rao, “*Majorana Dark Matter in a new B-L model,*” [arXiv:1710.05775](#).
- [37] K. Kannike, “*Vacuum Stability Conditions From Copositivity Criteria,*” *Eur. Phys. J.* **C72** (2012) 2093, [arXiv:1205.3781](#).
- [38] K. Kannike, “*Vacuum Stability of a General Scalar Potential of a Few Fields,*” *Eur. Phys. J.* **C76** (2016) no. 6, 324, [arXiv:1603.02680](#).
- [39] B. W. Lee, C. Quigg, and H. B. Thacker, “*Weak Interactions at Very High-Energies: The Role of the Higgs Boson Mass,*” *Phys. Rev.* **D16** (1977) 1519.
- [40] G. Belanger, B. Dumont, U. Ellwanger, J. F. Gunion, and S. Kraml, “*Status of invisible Higgs decays,*” *Phys. Lett.* **B723** (2013) 340–347, [arXiv:1302.5694](#).
- [41] P. P. Giardino, K. Kannike, I. Masina, M. Raidal, and A. Strumia, “*The universal Higgs fit,*” *JHEP* **05** (2014) 046, [arXiv:1303.3570](#).
- [42] S. Weinberg, “*Goldstone Bosons as Fractional Cosmic Neutrinos,*” *Phys. Rev. Lett.* **110** (2013) no. 24, 241301, [arXiv:1305.1971](#).
- [43] E. Ma, “*Verifiable radiative seesaw mechanism of neutrino mass and dark matter,*” *Phys. Rev.* **D73** (2006) 077301, [arXiv:hep-ph/0601225](#).
- [44] G. Blanger, K. Kannike, A. Pukhov, and M. Raidal, “*Minimal semi-annihilating Z_N scalar dark matter,*” *JCAP* **1406** (2014) 021, [arXiv:1403.4960](#).
- [45] S. Iso, N. Okada, and Y. Orikasa, “*The minimal B-L model naturally realized at TeV scale,*”

- Phys. Rev. **D80** (2009) 115007, [arXiv:0909.0128](#).
- [46] A. V. Semenov, “*LanHEP: A Package for automatic generation of Feynman rules in gauge models*,” [arXiv:hep-ph/9608488](#).
- [47] A. Pukhov, E. Boos, M. Dubinin, V. Edneral, V. Ilyin, D. Kovalenko, A. Kryukov, V. Savrin, S. Shichanin, and A. Semenov, “*CompHEP: A Package for evaluation of Feynman diagrams and integration over multiparticle phase space*,” [arXiv:hep-ph/9908288](#).
- [48] G. Belanger, F. Boudjema, A. Pukhov, and A. Semenov, “*MicrOMEGAs 2.0: A Program to calculate the relic density of dark matter in a generic model*,” *Comput. Phys. Commun.* **176** (2007) 367–382, [arXiv:hep-ph/0607059](#).
- [49] G. Belanger, F. Boudjema, A. Pukhov, and A. Semenov, “*Dark matter direct detection rate in a generic model with micrOMEGAs 2.2*,” *Comput. Phys. Commun.* **180** (2009) 747–767, [arXiv:0803.2360](#).
- [50] M. W. Goodman and E. Witten, “*Detectability of Certain Dark Matter Candidates*,” *Phys. Rev.* **D31** (1985) 3059.
- [51] G. Jungman, M. Kamionkowski, and K. Griest, “*Supersymmetric dark matter*,” *Phys. Rept.* **267** (1996) 195–373, [arXiv:hep-ph/9506380](#).
- [52] S. Khalil, H. Okada, and T. Toma, “*Right-handed Sneutrino Dark Matter in Supersymmetric B-L Model*,” *JHEP* **07** (2011) 026, [arXiv:1102.4249](#).
- [53] C.-W. Chiang, T. Nomura, and J. Tandean, “*Dark Matter and Higgs Boson in a Model with Discrete Gauge Symmetry*,” *Phys. Rev.* **D87** (2013) no. 7, 073004, [arXiv:1205.6416](#).
- [54] S. Kanemura, T. Nabeshima, and H. Sugiyama, “*TeV-Scale Seesaw with Loop-Induced Dirac Mass Term and Dark Matter from $U(1)_{B-L}$ Gauge Symmetry Breaking*,” *Phys. Rev.* **D85** (2012) 033004, [arXiv:1111.0599](#).
- [55] J.-M. Zheng, Z.-H. Yu, J.-W. Shao, X.-J. Bi, Z. Li, and H.-H. Zhang, “*Constraining the interaction strength between dark matter and visible matter: I. fermionic dark matter*,” *Nucl. Phys.* **B854** (2012) 350–374, [arXiv:1012.2022](#).
- [56] Y. Farzan and E. Ma, “*Dirac neutrino mass generation from dark matter*,” *Phys. Rev.* **D86** (2012) 033007, [arXiv:1204.4890](#).
- [57] K. Kohri and N. Sahu, “*Constraining theogenesis of visible and dark matter with AMS-02 and Xenon-100*,” *Phys. Rev.* **D88** (2013) 103001, [arXiv:1306.5629](#).
- [58] **XENON**, E. Aprile *et al.*, “*First Dark Matter Search Results from the XENON1T Experiment*,” [arXiv:1705.06655](#).
- [59] **LUX**, D. S. Akerib *et al.*, “*Results from a search for dark matter in the complete LUX exposure*,” *Phys. Rev. Lett.* **118** (2017) no. 2, 021303, [arXiv:1608.07648](#).
- [60] T. A. collaboration, “*Search for new phenomena in the dilepton final state using proton-proton collisions at $s = 13$ TeV with the ATLAS detector*,”.
- [61] A. Belyaev, N. D. Christensen, and A. Pukhov, “*CalcHEP 3.4 for collider physics within and beyond the Standard Model*,” *Comput. Phys. Commun.* **184** (2013) 1729–1769, [arXiv:1207.6082](#).
- [62] K. Kong, “*TASI 2011: CalcHEP and PYTHIA Tutorials*,” in *The Dark Secrets of the Terascale: Proceedings, TASI 2011, Boulder, Colorado, USA, Jun 6 - Jul 11, 2011*,

- pp. 161–198. 2013. [arXiv:1208.0035](https://arxiv.org/abs/1208.0035).
<https://inspirehep.net/record/1124593/files/arXiv:1208.0035.pdf>.
- [63] **DELPHI, OPAL, LEP Electroweak, ALEPH, L3**, S. Schael *et al.*, “*Electroweak Measurements in Electron-Positron Collisions at W-Boson-Pair Energies at LEP*,” Phys. Rept. **532** (2013) 119–244, [arXiv:1302.3415](https://arxiv.org/abs/1302.3415).
- [64] J. R. Ellis, A. Ferstl, and K. A. Olive, “*Reevaluation of the elastic scattering of supersymmetric dark matter*,” Phys. Lett. **B481** (2000) 304–314, [arXiv:hep-ph/0001005](https://arxiv.org/abs/hep-ph/0001005).
- [65] J. Schechter and J. W. F. Valle, “*Neutrino Decay and Spontaneous Violation of Lepton Number*,” Phys. Rev. **D25** (1982) 774.
- [66] M. Lindner, T. Ohlsson, and W. Winter, “*A Combined treatment of neutrino decay and neutrino oscillations*,” Nucl. Phys. **B607** (2001) 326–354, [arXiv:hep-ph/0103170](https://arxiv.org/abs/hep-ph/0103170).
- [67] F. D’Eramo and J. Thaler, “*Semi-annihilation of Dark Matter*,” JHEP **06** (2010) 109, [arXiv:1003.5912](https://arxiv.org/abs/1003.5912).
- [68] F. Calore, I. Cholis, C. McCabe, and C. Weniger, “*A Tale of Tails: Dark Matter Interpretations of the Fermi GeV Excess in Light of Background Model Systematics*,” Phys. Rev. **D91** (2015) no. 6, 063003, [arXiv:1411.4647](https://arxiv.org/abs/1411.4647).
- [69] T. Daylan, D. P. Finkbeiner, D. Hooper, T. Linden, S. K. N. Portillo, N. L. Rodd, and T. R. Slatyer, “*The characterization of the gamma-ray signal from the central Milky Way: A case for annihilating dark matter*,” Phys. Dark Univ. **12** (2016) 1–23, [arXiv:1402.6703](https://arxiv.org/abs/1402.6703).
- [70] P. Agrawal, B. Batell, P. J. Fox, and R. Harnik, “*WIMPs at the Galactic Center*,” JCAP **1505** (2015) 011, [arXiv:1411.2592](https://arxiv.org/abs/1411.2592).
- [71] **PAMELA**, O. Adriani *et al.*, “*Cosmic-Ray Positron Energy Spectrum Measured by PAMELA*,” Phys. Rev. Lett. **111** (2013) 081102, [arXiv:1308.0133](https://arxiv.org/abs/1308.0133).
- [72] **AMS**, M. Aguilar *et al.*, “*Electron and Positron Fluxes in Primary Cosmic Rays Measured with the Alpha Magnetic Spectrometer on the International Space Station*,” Phys. Rev. Lett. **113** (2014) 121102.
- [73] M. Boudaud *et al.*, “*A new look at the cosmic ray positron fraction*,” Astron. Astrophys. **575** (2015) A67, [arXiv:1410.3799](https://arxiv.org/abs/1410.3799).